FoxOs Enforce a Progression Checkpoint to Constrain mTORC1-Activated Renal Tumorigenesis

Boyi Gan,[1,2,3,4] Carol Lim,[1,2,3,4] Gerald Chu,[1,3,4,5] Sujun Hua,[1,2,3,4] Zhihu Ding,[1,2,3,4] Michael Collins,[5]
Jian Hu,[1,2,3,4] Shan Jiang,[1,2,3,4] Eliot Fletcher-Sananikone,[1,2,3,4] Li Zhuang,[1,2,3,4] Michelle Chang,[5] Hongwu Zheng,[1,2,3,4]
Y. Alan Wang,[1,2,3,4] David J. Kwiatkowski,[6] William G. Kaelin, Jr.,[2,3,7] Sabina Signoretti,[2,5] and Ronald A. DePinho[1,2,3,4,*]
[1]Belfer Institute for Applied Cancer Science
[2]Department of Medical Oncology, Dana-Farber Cancer Institute, Boston, MA 02115, USA
[3]Department of Medicine
[4]Department of Genetics, Harvard Medical School, Boston, MA 02115, USA
[5]Department of Pathology
[6]Division of Translational Medicine, Brigham and Women's Hospital, Boston, MA 02115, USA
[7]Howard Hughes Medical Institute, Chevy Chase, MD 20815, USA
*Correspondence: ron_depinho@dfci.harvard.edu
DOI 10.1016/j.ccr.2010.10.019

SUMMARY

mTORC1 is a validated therapeutic target for renal cell carcinoma (RCC). Here, analysis of *Tsc1*-deficient (mTORC1 hyperactivation) mice uncovered a FoxO-dependent negative feedback circuit constraining mTORC1-mediated renal tumorigenesis. We document robust FoxO activation in *Tsc1*-deficient benign polycystic kidneys and FoxO extinction on progression to murine renal tumors; murine renal tumor progression on genetic deletion of both *Tsc1* and *FoxOs*; and downregulated FoxO expression in most human renal clear cell and papillary carcinomas, yet continued expression in less aggressive RCCs and benign renal tumor subtypes. Mechanistically, integrated analyses revealed that FoxO-mediated block operates via suppression of Myc through upregulation of the Myc antagonists, Mxi1-SRα and mir-145, establishing a FoxO-Mxi1-SRα/mir-145 axis as a major progression block in renal tumor development.

INTRODUCTION

The mammalian target of rapamycin complex 1 (mTORC1) serves as the key regulator of protein synthesis and cell growth via phosphorylation of a variety of downstream targets, including S6 Kinase and 4E-BP1 (Ma and Blenis, 2009; Wullschleger et al., 2006), and plays a critical role in the regulation of cell growth, angiogenesis, and metabolism in many human cancers, including renal cell carcinoma (RCC) (Guertin and Sabatini, 2006, 2007; Hanna et al., 2008; Inoki et al., 2005). RCC comprises ~3% of all adult malignancies, ranks among the top 10 cancers in the United States, and continues to show modest responses to most conventional cancer treatments (Linehan and Zbar, 2004; Rini et al., 2009). mTORC1 hyperactivation is observed in the majority of human RCC samples (Pantuck et al., 2007; Robb et al., 2007) and has emerged as a therapeutic target for RCC after several clinical trials establishing clinical benefit of mTORC1 inhibitors (Atkins et al., 2004; Hudes et al., 2007; Motzer et al., 2008). Given the clinical relevance of the mTORC1 target in RCC, an understanding of mTORC1's complex signaling circuitry in vivo may inform its role in RCC pathogenesis and guide further drug development efforts.

Significance

The clinical response of RCC to mTORC1 inhibition has been modest. The clinical application of mTORC1 inhibitors may be improved by the development of mTORC1-directed mouse models of RCC and by illumination of the mTORC1 activation network in RCC pathogenesis. This study reports the engineering of a highly penetrant model of renal adenoma/carcinoma and identification of a FoxO-Myc network as integral regulators of renal tumorigenesis in mice and humans. Illumination of this circuit may provide strategies to understand the variable clinical response to mTORC1 inhibition in RCC patients and motivate the development of combination treatment by mTORC1 inhibitors and agents reactivating FoxO or targeting Myc in human RCC.

Increasing knowledge of mTORC1 signaling has demonstrated that mTORC1 acts both downstream and upstream of PI3K-AKT signaling. Whereas activated PI3K-AKT signaling promotes mTORC1 signaling through AKT-mediated phosphorylation of both TSC2 and PRAS40, mTORC1 hyperactivation also leads to feedback shutoff of PI3K/AKT signaling via a S6 Kinase-dependent downregulation of upstream activators of PI3K including the PDGF receptor and IRS-1 (Bhaskar and Hay, 2007; Guertin and Sabatini, 2007; Hay and Sonenberg, 2004; Manning, 2004; Um et al., 2006). A major upstream regulator of mTORC1 is the TSC1-TSC2 complex, which functions to inhibit the mTORC1 activity via stimulation of GTP hydrolysis and inactivation of small GTPase Rheb, an activator of mTORC1 (Huang and Manning, 2008; Kwiatkowski and Manning, 2005; Li et al., 2004). These observations hold important therapeutic implications in that, in specific genotypic contexts, mTORC1 inhibitor treatment alone might enhance tumorigenesis in mTORC1 hyperactivation-driven tumors by stimulating PI3K-AKT-dependent survival and cell cycle entry, thereby prompting calls for combination therapeutic regimens in the clinic (Shaw and Cantley, 2006). Along these lines, the rational design and effective implementation of such combinations requires a more definitive understanding of the key downstream effector(s) of AKT that mediate this mTORC1-directed negative feedback circuit.

The PI3K-AKT axis is activated in virtually all human cancers (Cully et al., 2006; Luo et al., 2003; Salmena et al., 2008; Samuels et al., 2004). The wide range of tumorigenic phenotypes mediated by PI3K-AKT signaling is consistent with the existence of diverse downstream effectors including TSC1-TSC2 complex, FoxOs, GSK3 and MDM2. These effectors operate in a highly context-specific manner, i.e., effectors are coordinately or differentially used in conferring neoplastic phenotypes in distinct cell lineages and genotypes (Manning and Cantley, 2007). The mammalian FoxO transcription factors—FoxO1, FoxO3, FoxO4—function in the nucleus to direct transcription of specific gene targets governing cellular survival, proliferation, metabolism, differentiation, and oxidative defense. Activation of PI3K by extracellular growth factors leads to AKT-mediated phosphorylation of FoxO1, FoxO3, and FoxO4, resulting in their sequestration in the cytoplasm such that they are unable to regulate their gene targets (Accili and Arden, 2004; Greer and Brunet, 2005). The role and essentiality of the FoxOs in tumor suppression in vivo has received formal proof from murine genetic studies wherein broad somatic deletion of all three *FoxOs* was shown to engender a cancer-prone condition dominated by hemangiomas and lymphomas (Paik et al., 2007). However, the highly context and cell-lineage specific functions of FoxO as revealed from this study also highlights the necessity to fully characterize its tumor suppression function in other cell types and tissue contexts. We studied FoxO tumor suppression function in the context of mTORC1-mediated renal tumorigenesis.

RESULTS

FoxOs Are Activated in *Tsc1*-Deficient Polycystic Kidneys, but Lost in *Tsc1*-Deficient Renal Adenomas and Carcinomas

To better understand the molecular and biological role of mTORC1 hyperactivation in renal cancer development, we assessed the impact of homozygous deletion of *Tsc1* conditional knockout (KO) allele (*Tsc1^L^*) (Kwiatkowski et al., 2002) using the *Rosa26-CreERT2* knock-in deletor allele that enables tamoxifen-inducible Cre-mediated excision of conditional knockout alleles in most tissues, including kidneys (Vooijs et al., 2001). Tamoxifen-treatment of adult *Tsc1^L/L^*, *Rosa26-CreERT2* mice resulted in efficient deletion of *Tsc1* in the kidney (see Figures S1A and S1B available online) as well as other organs (data not shown). As recently reported (Gan et al., 2008), somatic deletion of *Tsc1* in adult mice (*Tsc1^L/L^*, *Rosa26-CreERT2*, hereafter referred to as "*Tsc1* KO") led to the development of polycystic kidney disease (Figures 1Aa–1Ac), as well as severe hematopoietic defects (data not shown) compared with littermate "*Tsc1* wild-type (WT)" control mice (*Tsc1^L/L^* or *Tsc1^+/+^*, *Rosa26-CreERT2* mice treated with tamoxifen). All *Tsc1* KO mice developed severe renal and bone marrow failure and died within 7 weeks (Gan et al., 2008). Notably, all *Tsc1* KO mice developed bilateral polycystic kidneys with >10-fold weights relative to littermate controls (Figure 1Ac) and significantly dilated renal tubules on histopathological analysis (Figures 1Aa and 1Ab), which is consistent with the documented connection between tuberous sclerosis and polycystic kidney disease (Cai and Walker, 2006).

The *Tsc1* KO polycystic kidneys exhibited increased phospho-S6 staining compared with WT kidneys (Figure S1C), and rapamycin treatment of *Tsc1* KO mice resulted in full rescue of the polycystic kidney defect (data not shown), strongly suggesting that mTORC1 hyperactivation upon loss of *Tsc1* drives the polycystic kidney phenotype in the *Tsc1* KO model. Given the lethality of the *Tsc1* KO mice, we also established a large cohort of *Tsc1^L/+^*, *Rosa26-CreERT2* mice (hereafter referred to as "*Tsc1^+/−^*") for long-term tumor studies. Consistent with previous reports from mice heterozygous for germ line *Tsc1* null allele (Kobayashi et al., 2001; Kwiatkowski et al., 2002), our conditional *Tsc1^+/−^* model showed renal adenomas and/or carcinomas after long latency (>14 months) (Figures 1Ad and 2B). These renal adenomas and carcinomas demonstrated loss of heterozygosity (LOH) for the remaining *Tsc1* allele (six of six samples examined; data not shown) as well as increased phospho-S6 staining indicative of mTORC1 hyperactivation (Figure 1C).

The long latency required for the development of *Tsc1*-deficient renal carcinomas prompted us to consider that this model could prove useful in the identification of physiologically relevant checkpoint pathways activated in *Tsc1* KO premalignant polycystic kidneys and enable the validation of such checkpoints through a detailed comparative analysis of activation status of TSC-mTORC1-related signaling surrogates in *Tsc1*-deficient polycystic lesions versus tumor samples. These comparative analyses revealed strong FoxO1 and FoxO3 staining with predominant nuclear localization (Figure 1B), a pattern consistent with strong FoxO activation in *Tsc1* KO polycystic kidneys relative to WT kidney samples.

In line with these tissue findings, *Tsc1* and *Tsc2* KO MEFs exhibited decreased FoxO1/3 phosphorylation compared with WT MEFs (Figure S1D) and, accordingly, showed predominant FoxO1/3 nuclear localization under both serum starvation and stimulation conditions (Figure S1E). This profile corresponds well with the anticipated constitutively high mTORC1 activity and dramatically reduced AKT phosphorylation in *Tsc*-deficient
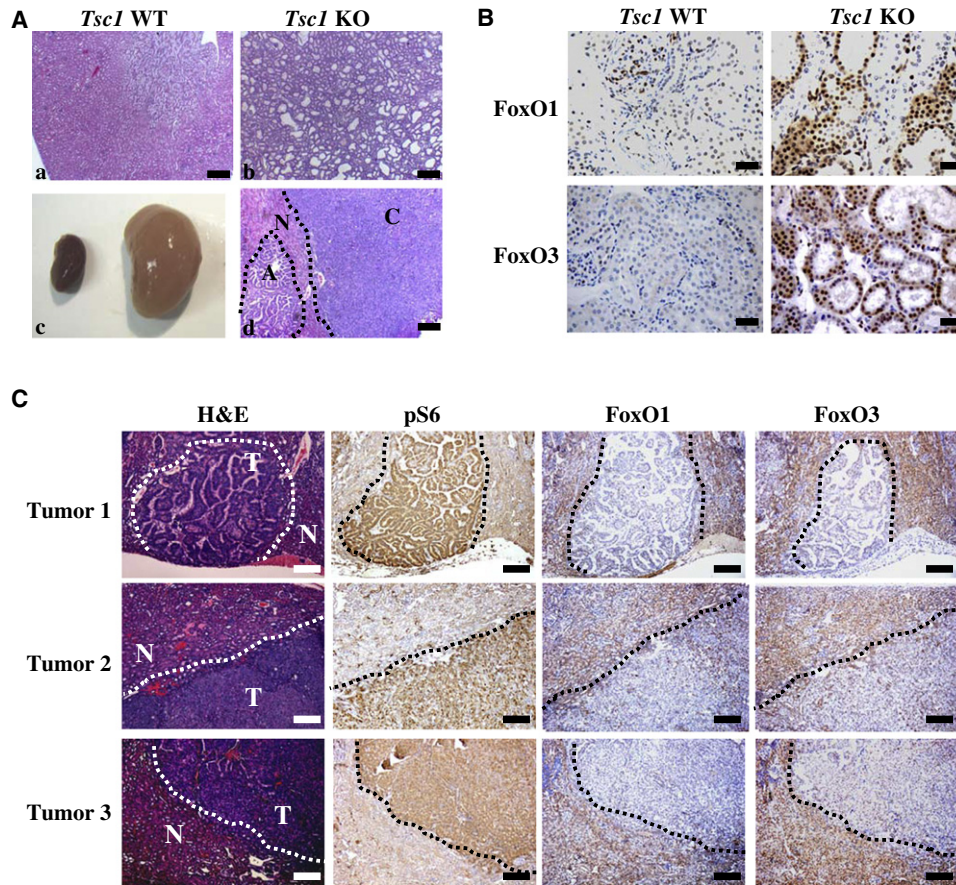
Figure 1. FoxOs Are Activated in *Tsc1*-Deficient Polycystic Kidneys, but Lost in *Tsc1*-Deficient Renal Adenomas and Carcinomas

(A) Gross view of *Tsc1* WT (left) and KO kidneys (right) at 30 days post-tamoxifen injection (DPI) at 9 weeks of age (c), hematoxylin and eosin (H&E) staining of *Tsc1* WT and KO kidney sections (a and b), and *Tsc1*-deficient kidney tumors (d). C: carcinoma; A: adenoma; N: surrounding normal kidney cells. Scale bars, 200 μm.

(B) Immunohistochemical staining of *Tsc1* WT and KO kidney sections with antibodies against FoxO1 and FoxO3, showing predominant nuclear localization of FoxO1 and FoxO3 in *Tsc1* KO kidneys compared with WT kidneys. Scale bars, 20 μm.

(C) H&E and immunohistochemical staining of *Tsc1* KO renal tumors with antibodies against phospho S6, FoxO1, and FoxO3, showing increased phospho S6 staining and marked reduction or absence of FoxO1 and FoxO3 staining in *Tsc1*-deficient renal tumors compared with adjacent normal kidney cells. In H&E staining sections, "T" denotes tumor region, and "N" denotes adjacent normal kidney region. Scale bars, 100 μm. See also Figure S1.

MEFs (Figure S1D). On this basis, we considered a model in which the regulation of FoxO activity might play a critical effector role in the mTORC1-AKT negative feedback circuit and that FoxO extinction would promote tumorigenesis. In line with this hypothesis, we observed marked reduction/loss of both FoxO1 and FoxO3 staining in all *Tsc1* KO renal adenoma/carcinoma samples examined (10 of 10 bilateral kidneys, each with multiple renal adenomas/carcinomas) compared with surrounding nonmalignant cells (Figure 1C). Furthermore, western blotting analysis revealed significant reduction of FoxO4 protein levels in *Tsc1*-deficient renal tumors compared with adjacent normal kidney samples (Figure S1F). Together, these data are consistent with the possibility that FoxO activation participates in a feedback checkpoint functioning to restrain the renal tumorigenesis initiated by loss of *Tsc1*, and that subsequent loss of *FoxO* may be required for renal cancer development in *Tsc1*-deficient mice.
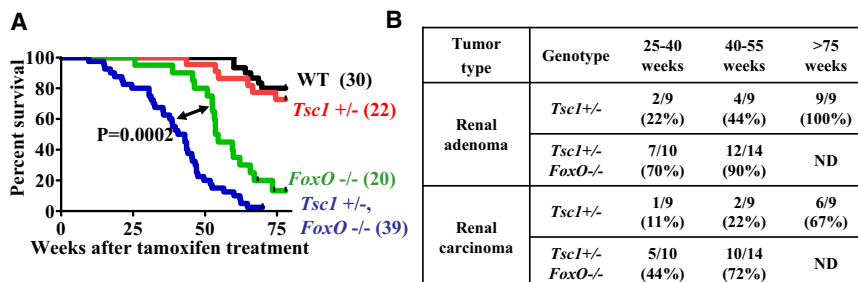

Figure 2. Dual Inactivation of *FoxO* and *Tsc1* Dramatically Drives Renal Tumor Progression

(A) Kaplan-Meier overall survival analysis for mice of indicated genotypes as a function of weeks after tamoxifen treatment. Cohort size for each mice colony is also indicated.

(B) Table showing the incidence of renal adenoma and carcinoma in *Tsc1*^{+/−} and *Tsc1*^{+/−} *FoxO*^{−/−} mice at various stages. ND: not determined.

Tumor type	Genotype	25-40 weeks	40-55 weeks	>75 weeks
Renal adenoma	*Tsc1+/-*	2/9 (22%)	4/9 (44%)	9/9 (100%)
	Tsc1+/- FoxO-/-	7/10 (70%)	12/14 (90%)	ND
Renal carcinoma	*Tsc1+/-*	1/9 (11%)	2/9 (22%)	6/9 (67%)
	Tsc1+/- FoxO-/-	5/10 (44%)	10/14 (72%)	ND

Dual Inactivation of *FoxO* and *Tsc1* Dramatically Drives Renal Tumor Progression

To secure genetic evidence for the hypothetical FoxO-dependent block of *Tsc1* KO renal carcinoma development, we engineered mice harboring conditional knockout alleles of *Tsc1* and/or *FoxO1/3/4*, and *Rosa26-CreERT2*. (For simplicity, after tamoxifen treatment to induce gene deletion, "*FoxO1/3/4^{L/L}*, *Rosa26-CreERT2*" mice will be referred to as "*FoxO^{−/−}*" hereafter.) We established *Tsc1^{+/+} FoxO^{+/+}* (WT), *Tsc1^{+/−} FoxO^{−/−}*, *Tsc1^{+/−} FoxO^{+/+}*, and *Tsc1^{+/+} FoxO^{−/−}* cohorts and monitored survival and cancer predisposition over a period of 80 weeks. Although there was no significant survival difference between *Tsc1^{+/−}* and WT mice, there was a marked *Tsc1*-dependent reduction in lifespan of *FoxO^{−/−}* mice (*FoxO^{−/−}* mean survival 54.1 weeks versus *Tsc1^{+/−} FoxO^{−/−}* mean survival 41.8 weeks, p = 0.0002) (Figure 2A). The decrease in survival in *FoxO^{−/−}* mice relates to hemangiosarcomas and thymic lymphomas as previously reported (Paik et al., 2007) and careful inspection of the kidneys showed no evidence of renal adenoma or carcinoma (data not shown). In contrast, *Tsc1^{+/−} FoxO^{−/−}* mice showed dramatic reduction in latency and increased penetrance of renal adenomas and carcinomas (Figure 2B). Notably, the penetrance and onset of *FoxO^{−/−}* cancer phenotypes (hemangiosarcomas and thymic lymphomas) were not affected in *Tsc1^{+/−} FoxO^{−/−}* mice. The accelerated renal tumor development in *Tsc1^{+/−} FoxO^{−/−}* mice significantly contributed to the shorter life span of *Tsc1^{+/−} FoxO^{−/−}* mice compared with *FoxO^{−/−}* mice. These genetic studies establish that FoxO activation is a potent block in *Tsc1* null renal tumor development in the in vivo setting.

FoxOs Are Extinguished in the Majority of Human Renal Tumor Samples

The above data from murine model systems prompted detailed examination of FoxO expression/activation status in human kidney tumor samples. RCC is the most common malignancy of the adult kidney and presents as a heterogeneous group of tumors with distinct histological features, including clear cell, papillary (including both type 1 and type 2), and chromophobe RCC as well as rarer subtypes (Lopez-Beltran et al., 2006). Clear cell RCC (ccRCC) is the predominant subtype and accounts for up to 75% of total RCC cases (Linehan and Zbar, 2004; Rini et al., 2009). It is generally considered that all the clear-cell tumors are carcinomas, with greater or lesser aggressiveness, and an adenoma state of clear cells is not accepted (Algaba, 2008). Compared with more aggressive clear cell and papillary subtypes, chromophobe RCCs tend to have a benign course after surgery, provided that the tumor stage and grade are favorable at the time of surgery (Cohen and McGovern, 2005). Benign epithelial neoplasms also occur in the kidney, including oncocytoma and metanephric adenoma, among others.

To assess FoxO expression in this spectrum of benign and aggressive kidney tumor types, FoxO1 and FoxO3 protein abundance was determined by immunohistochemistry (IHC) in a tissue microarray (TMA) that contained 21 normal kidney samples, 68 clear cell RCC, 10 papillary RCC, 8 chromophobe RCC, 5 oncocytomas, as well as several rare renal tumor subtypes. TMA-IHC analysis revealed FoxO1 and FoxO3 cytoplasmic and nuclear signal in both the proximal and distal tubular epithelium in normal kidney samples (Figures 3Aa and 3Ca). In contrast, FoxO1 and FoxO3 signal was not detectable in the majority of clear cell and papillary RCC samples (FoxO1: 64 of 68 clear cell and 8 of 10 papillary; FoxO3: 63 of 68 clear cell and 7 of 10 papillary) (Figures 3A–3D). FoxO1 and FoxO3 signal was readily detected in the tumor endothelial cells, providing a positive internal staining control (Figure S2A; data not shown). Notably, all of the less aggressive RCCs and benign renal tumors retained FoxO1 and/or FoxO3 expression (Figures 3A–3D). FoxO1 nuclear signal was especially strong in oncocytoma samples (Figure S2B).

We also assessed phospho-S6 staining on the same TMA sample set. This analysis revealed negative to weak phospho-S6 staining in most normal kidney samples and moderate to strong phospho-S6 staining in the majority of human renal clear cell and papillary carcinomas samples (Figures 3E and 3F), consistent with previous reports that mTORC1 hyperactivation is observed in the majority of human RCC samples (Pantuck et al., 2007; Robb et al., 2007). Importantly, our analysis also showed negative to weak phospho-S6 staining in chromophobe RCC, oncocytoma and metanephric adenoma samples (Figures 3E and 3F). The inverse staining pattern between FoxO1/3 and phospho-S6 from different human renal tumor types provides further support to our conclusion that FoxOs serve as a checkpoint in mTORC1-activated renal tumorigenesis.

FoxO Activation Promotes Cell Cycle Arrest and Apoptosis in Human RCC Cells

The above data prompted further examination of FoxO function in human RCC cell lines. We first examined the expression levels of FoxO1/3 and mTORC1 activation status in a panel of human RCC cell lines and the immortalized WT human kidney cells (HK2). Consistent with the data from murine renal tumors (Figure 1C), these analyses revealed that high phosphorylation levels of S6 (surrogate of mTORC1 activation) in general correlated with low expression levels of FoxO1 and FoxO3 in these human RCC cell lines (Figure 4A). We then assessed the impact of FoxO reactivation in RCC4 and UMRC2 cells that harbor low FoxO1/3 expression and high mTORC1 activation. To this end, we generated RCC4 and UMRC2 cell lines with stable expression of FoxO1(TA)ERT2 or FoxO3(TA)ERT2 construct, which expressed a fusion protein consisting of FoxO(TA) (containing three Ser/Thr AKT phosphorylation sites mutated to alanine) fused to the T2-modified estrogen receptor (ERT2) moiety (Figure S3A). We documented that FoxO(TA)ERT2 fusion protein sequestered FoxO(TA) in the cytoplasm and that 4OHT treatment resulted in rapid translocation of FoxO(TA)ERT2 into nucleus (Figure S3B). We also established stable cell lines with ERT2 expression as control cell lines. (For simplicity, ERT2, FoxO1(TA)ERT2, and FoxO3(TA)ERT2 cell lines will be referred to as empty vector [EV], FoxO1, and FoxO3 thereafter.) 4OHT treatment of FoxO1 or FoxO3 RCC4 cells resulted in marked cell growth suppression compared with vehicle-treated cells or 4OHT-treated EV RCC4 cells (Figures 4B and 4C). Further analysis demonstrated that FoxO reactivation in RCC4 cells led to potent G1/S cell cycle arrest (Figure 4D) and enhanced apoptosis (Figure 4E). Reactivation of FoxO1/3 in UMRC2 cells resulted in similar phenotypes (Figures S3C–S3E). Finally, in UOK101 cells that maintain FoxO3 and FoxO1 expression, knockdown of both FoxO1 and FoxO3 led to increased cell proliferation (Figures 4F and 4G).
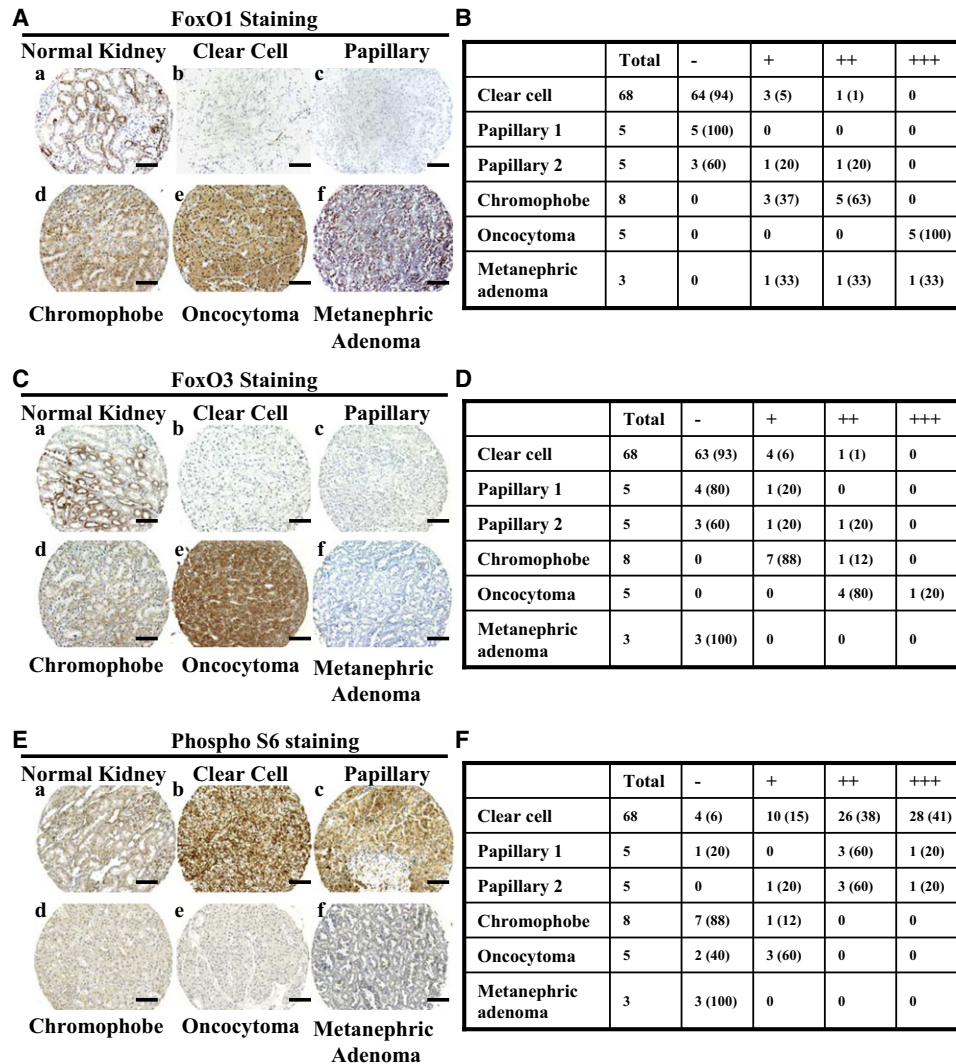
A FoxO1 Staining

B

	Total	-	+	++	+++
Clear cell	68	64 (94)	3 (5)	1 (1)	0
Papillary 1	5	5 (100)	0	0	0
Papillary 2	5	3 (60)	1 (20)	1 (20)	0
Chromophobe	8	0	3 (37)	5 (63)	0
Oncocytoma	5	0	0	0	5 (100)
Metanephric adenoma	3	0	1 (33)	1 (33)	1 (33)

C FoxO3 Staining

D

	Total	-	+	++	+++
Clear cell	68	63 (93)	4 (6)	1 (1)	0
Papillary 1	5	4 (80)	1 (20)	0	0
Papillary 2	5	3 (60)	1 (20)	1 (20)	0
Chromophobe	8	0	7 (88)	1 (12)	0
Oncocytoma	5	0	0	4 (80)	1 (20)
Metanephric adenoma	3	3 (100)	0	0	0

E Phospho S6 staining

F

	Total	-	+	++	+++
Clear cell	68	4 (6)	10 (15)	26 (38)	28 (41)
Papillary 1	5	1 (20)	0	3 (60)	1 (20)
Papillary 2	5	0	1 (20)	3 (60)	1 (20)
Chromophobe	8	7 (88)	1 (12)	0	0
Oncocytoma	5	2 (40)	3 (60)	0	0
Metanephric adenoma	3	3 (100)	0	0	0

Figure 3. FoxOs Are Extinguished in the Majority of Human Renal Tumor Samples

(A, C, and E) Representative immunohistochemical images showing FoxO1 (A), FoxO3 (C), and phospho-S6 (E) staining in normal kidney and different subtypes of RCC samples from the TMA-IHC analysis. Scale bars, 50 μm.

(B, D, and F) Tables showing the number of tumor samples with corresponding staining scores of FoxO1 (B), FoxO3 (D), and phospho-S6 (F) in different subtypes of RCC samples. Percentage is shown in parenthesis. −, negative staining; +, low staining; ++, moderate staining; +++, strong staining. See also Figure S2.

These human RCC cell line data align with our murine data, strongly supporting the view that FoxOs function as tumor suppressors in the progression to human RCC.

Myc Signaling Is the Key Downstream Effector of FoxOs in the Regulation of Renal Tumorigenesis

We next sought to determine the mechanisms by which FoxO might govern the biology of RCC cells. To this end, we conducted comparative transcriptome analysis of EV, FoxO1, or FoxO3-expressing RCC4 and UMRC2 cells at 12 hr with or without 4OHT treatment. To enrich for more proximal actions of FoxO, we selected the 12-hr time point as time course studies revealed dramatic transcriptional changes of known FoxO targets (such as Cyclin D1), yet no discernible cellular phenotypes (apoptosis and cell cycle arrest) (data not shown). We generated four transcriptome data sets: FoxO1 RCC4, FoxO3 RCC4, FoxO1 UMRC2, and FoxO3 UMRC2, and normalized these transcriptome data against 4OHT-treated EV cells that show modest 4OHT-induced transcriptional changes (Figure 5A). As FoxO1 or FoxO3 reactivation generated comparable phenotypes, we further intersected FoxO1 and FoxO3 transcriptome data sets and focused on 503 genes exhibiting similar changes (designated as "FoxO RCC transcriptome"; Figure 5B; Table S1).

Next we conducted GSEA to identify gene sets that are enriched in FoxO RCC transcriptome. This analysis readily identified FoxO (TTGTTT_V$FOXO4_01), hypoxia (MANALO_HYPOXIA_DN) (Manalo et al., 2005), and E2F (V$E2F_Q6_01) gene sets in FoxO RCC transcriptome (Figure 5C; see Figure S4A for gene set description). Most notably, the analysis revealed
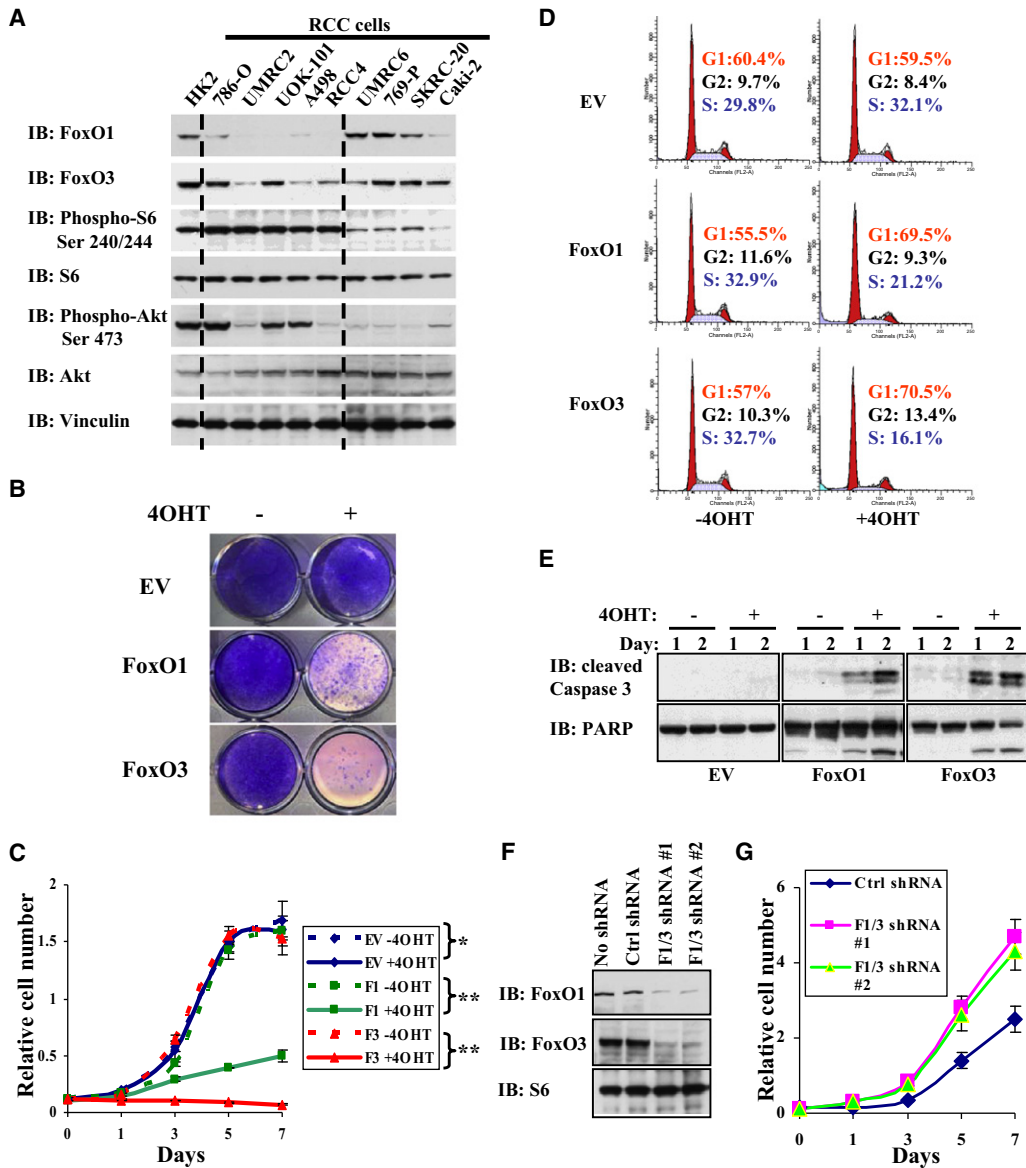
Figure 4. FoxO Activation Promotes Cell Cycle Arrest and Apoptosis in Human RCC Cells

(A) FoxO1/3 expression and mTORC1 activation status in human RCC cells. Western blotting by various antibodies was performed on cell lysates isolated from HK2 normal kidney cells and a panel of human RCC cell lines as indicated.

(B) Image showing the crystal violet staining of RCC4 EV, RCC4 FoxO1, RCC4 FoxO3 cells with or without 4OHT treatment for 7 days. EV, empty vector.

(C) Cell proliferation assay of RCC4 EV, RCC4 FoxO1, RCC4 FoxO3 cells with or without 4OHT treatment. *p > 0.5; **p = 6.6 × 10^{-5} (all refer to p values at day 7). Data are shown as mean ± SD from at least two independent experiments with triplicates.

(D) FACS analysis showing the cell cycle profiling of RCC4 EV, RCC4 FoxO1 (F1), RCC4 FoxO3 (F3) cells with or without 4OHT treatment for 2 days.

(E) RCC4 EV, RCC4 FoxO1, RCC4 FoxO3 cells were treated with or without 4OHT for 1 or 2 days as indicated. Cell lysates were then analyzed by western blotting with cleaved Caspase-3 and PARP as indicated.

(F) UOK101 cells were infected with ctrl (scramble) shRNA, FoxO1, and FoxO3 shRNA #1, or FoxO1 and FoxO3 shRNA #2-containing lentivirus. Cell lysates were extracted from stable cell lines and analyzed by western blotting with FoxO1, FoxO3, and S6 as indicated.

(G) Cell proliferation assay of UOK101 ctrl shRNA cells, UOK101 FoxO1/3 shRNA #1 cells, and UOK101 FoxO1/3 shRNA #2 cells. p < 10^{-4} for comparison between ctrl shRNA and F1/3 shRNA cells (all refer to p values at day 7). Data are shown as mean ± SD from two independent experiments with triplicates. See also Figure S3.

a previously described Myc oncogenic signature (Bild et al., 2006) as the most significantly enriched gene set (p = 4.51 × 10^{-16}; Figure 5C and Figure S4A). Accordingly, Myc binding motif-containing gene set (CACGTG_V$MYC_Q2) was also significantly enriched in FoxO RCC transcriptome (Figure 5C and Figure S4A). The connection of FoxO to Myc signaling in the context of RCC development is intriguing given recurrent *Myc* gene amplification in human RCC (Beroukhim et al.,
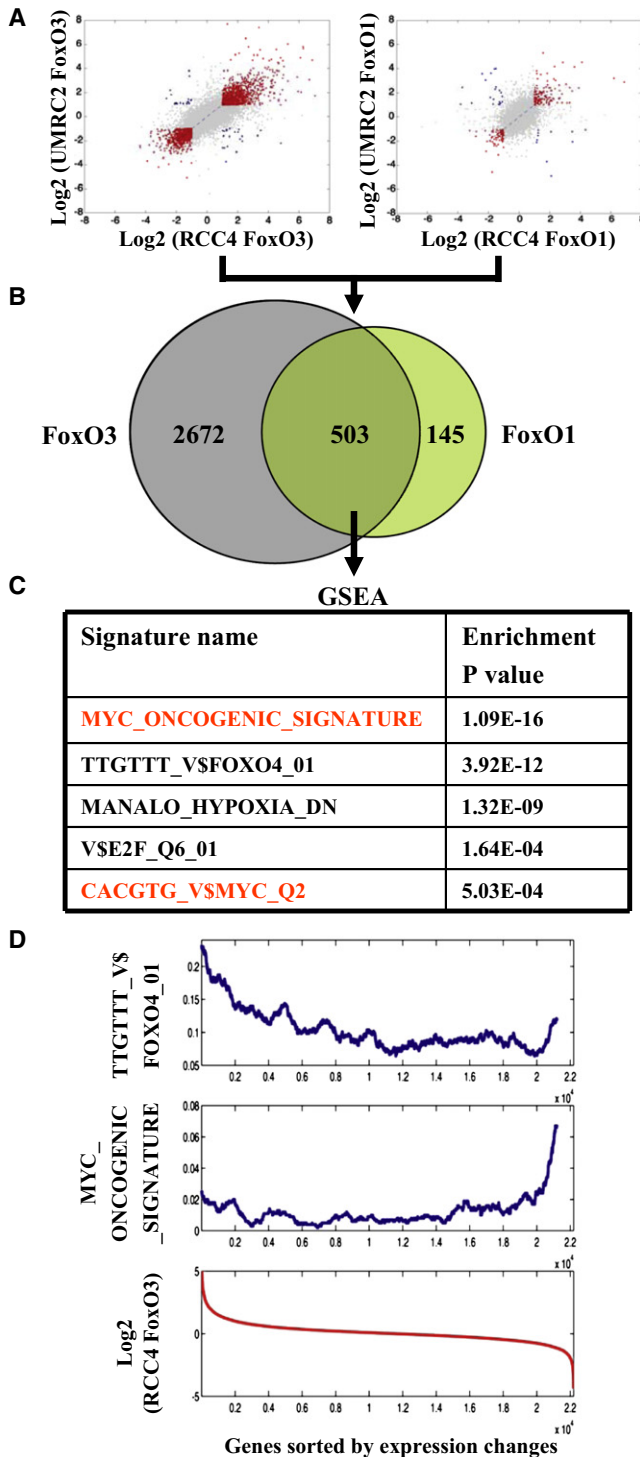
Figure 5. Myc Signaling Is the Key Downstream Effector of FoxOs in the Regulation of Renal Tumorigenesis

(A) Comparison of gene expression changes between RCC4 FoxO3 and UMRC2 FoxO3, RCC4 FoxO1 and UMRC2 FoxO1 transcriptome data sets. x and y axes show Log2 transformed fold changes in gene expression. Genes with fold changes >1.5 or <0.67 for both x and y axes are highlighted (with changes in the same direction in red and the opposite direction in blue, respectively).

2009), the involvement of Myc signaling in renal neoplasia as evidenced in genetically engineered mouse models (Schreiber-Agus et al., 1998; Trudel et al., 1991) and human cell culture studies (Eilers and Eisenman, 2008; Gordan et al., 2007a; Zhang et al., 2007) (see Discussion). To understand how FoxO might intersect with Myc signaling, we first considered a model wherein FoxO and Myc might coregulate a common set of transcription targets through cobinding on the same promoters. In silico promoter analysis of FoxO RCC transcriptome identified 90 putative FoxO direct targets and 81 putative Myc direct targets. However, integration of these two data sets only revealed 12 common targets, which is statistically insignificant (p > 0.5) (Figure S4B). Furthermore, the computational analysis showed that the FoxO putative targets (TTGTTT_V$FOXO4_01) are enriched in upregulated genes of the FoxO RCC transcriptome, whereas Myc signature genes (MYC_ONCOGENIC_SIGNATURE) are mostly enriched in downregulated genes of the FoxO RCC transcriptome (Figure 5D), suggesting FoxO might function to inhibit Myc activity and/or expression.

FoxOs Regulate Myc through Mxi-1 and mir-145 in RCC Cells

We and others previously showed that Mxi1 splicing variant strong repressor (Mxi1-SRα), but not Mxi1 weak repressor (Mxi1-WR), mediates antagonistic actions on Myc activity through recruitment of Sin3A-HDAC transcriptional repressor complex (Alland et al., 1997; Ayer et al., 1995; Heinzel et al., 1997; Schreiber-Agus et al., 1995). Mxi1-SRα was identified to be a FoxO direct target in other cellular contexts (Delpuech et al., 2007). We found FoxO activation significantly upregulated Mxi1-SRα expression while downregulating Mxi1-WR expression in both RCC4 and UMRC2 cells (Figures 6A and 6B; Figures S5A and S5B), suggesting FoxO might inhibit Myc activity via upregulation of Mxi1-SRα expression.

In addition, we observed FoxO reactivation resulted in significant downregulation of Myc expression in the FoxO RCC transcriptome and in confirmatory quantitative RT-PCR and western blot analysis of RCC4 cells and UMRC2 cells (Figures 6C and 6D; Figure S5C). The absence of FoxO binding elements in the Myc promoter region prompted us to consider that FoxO may regulate microRNA(s) governing Myc expression. To test this hypothesis, we examined the FoxO RCC transcriptome for enrichment of putative targets of microRNA genes, searched the microRNA promoter regions for putative FoxO binding elements (BEs), and determined whether any of these microRNAs could also target Myc via the targetScan algorithm and literature mining. This effort identified mir-145 that is known to target Myc (Sachdeva et al., 2009) and harbors 2 putative FoxO BEs within 2 kb

(B) Venn diagram displaying common transcriptome changes of FoxO1 and FoxO3 transcriptome data sets.
(C) The table showing the top lists of gene signatures enriched in FoxO RCC transcriptome data set with enrichment p value indicated.
(D) The distribution of putative FoxO targets (TTGTTT_V$FOXO4_01) and Myc-regulated genes (MYC_ONCOGENIC_SIGNATURE) in RCC4 FoxO3 transcriptome data set. All genes were sorted according to expression changes in RCC4 FoxO3 transcriptome data set (the red curve). The frequency of either putative FoxO targets (TTGTTT_V$FOXO4_01) or Myc-regulated genes (MYC_ONCOGENIC_SIGNATURE) in a sliding window of 1,000 sorted genes was calculated. See also Figure S4 and Table S1.
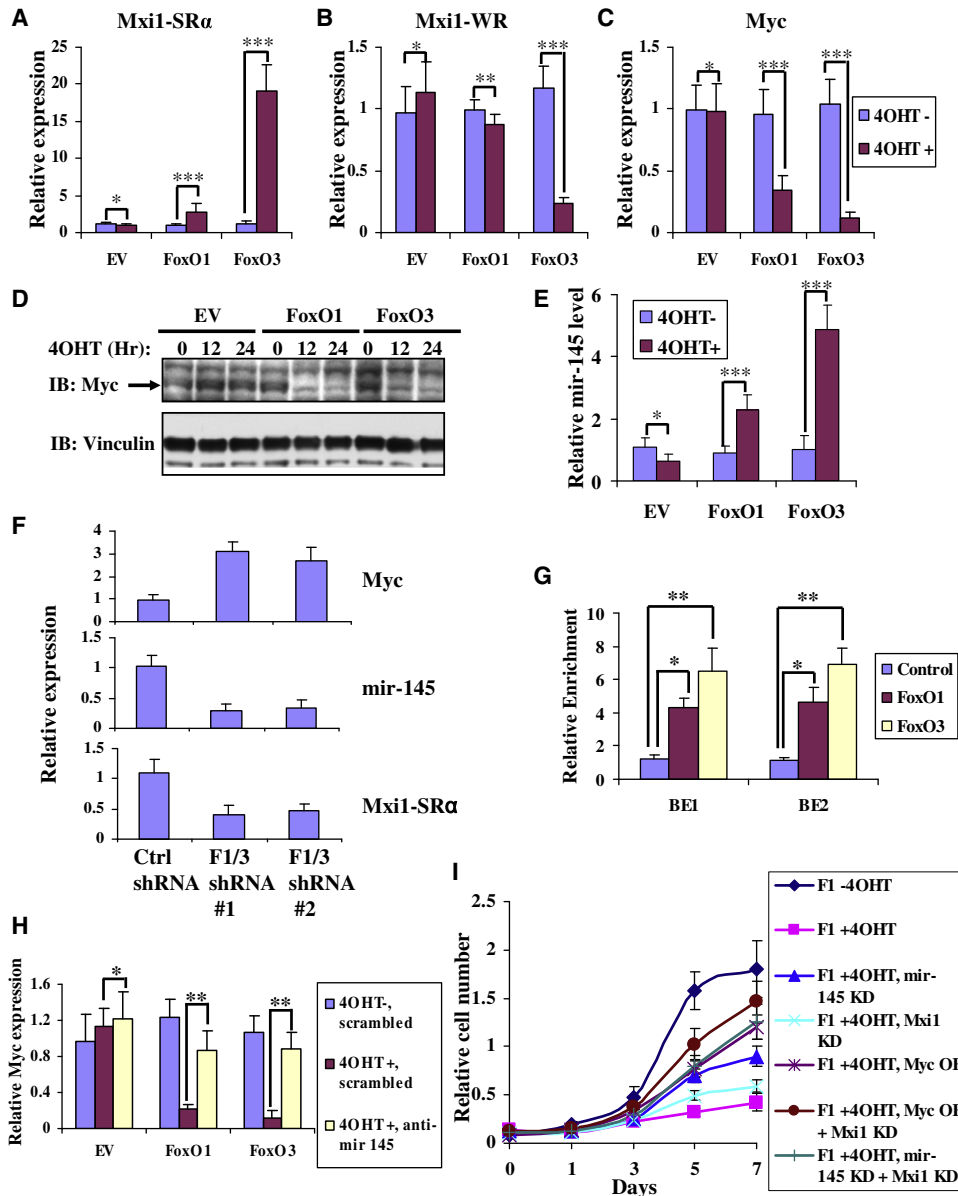
Figure 6. FoxOs Regulate Myc through Mxi-1 and mir-145 in RCC Cells

(A, B, C, and E) Bar graph showing the relative expression changes of Mxi1-SRα (A), Mxi1-WR (B), Myc (C), and mir-145 (E) by quantitative RT-PCR in RCC4 EV, RCC4 FoxO1, and RCC4 FoxO3 cells with or without 4OHT treatment for 12 hr. *p > 0.1; **p = 0.04; ***p < 0.01. Data are shown as mean ± SD from two independent experiments with triplicates.

(D) Western blotting showing endogenous Myc protein levels in RCC4 EV, RCC4 FoxO1, RCC4 FoxO3 cells at different time points after 4OHT treatment.

(F) Bar graph showing the relative expression changes of Myc, Mxi1-SRα, and mir-145 by quantitative RT-PCR in UOK101 ctrl shRNA cells, UOK101 FoxO1/3 shRNA #1 cells, and UOK101 FoxO1/3 shRNA #2 cells. p < 0.05 for comparison between ctrl shRNA and F1/3 shRNA cells in each setting. Data are shown as mean ± SD from two independent experiments with triplicates.

(G) Endogenous FoxO1 and FoxO3 directly bind to two FoxO BEs located in mir-145 promoter region in UOK101 cells. Bar graph showing the relative enrichment determined by quantitative RT-PCR after ChIP analysis using IgG (control), FoxO1 and FoxO3 antibodies. *p = 0.03; **p = 0.01. Data are shown as mean ± SD from two independent experiments with triplicates.

(H) mir-145 contributes to FoxO-mediated suppression of Myc expression in RCC4 cells. Bar graph showing the relative expression levels of endogenous Myc by quantitative RT-PCR in RCC4 EV, RCC4 FoxO1 or RCC4 FoxO3 cells with anti-mir-145 or scrambled control oligo transfection. *p > 0.5; **p < 0.01. Data are shown as mean ± SD from two independent experiments with triplicates.

(I) Cell proliferation assay of RCC4 FoxO1 (F1) cells under different conditions as indicated. OE: overexpression; KD: knockdown. Data are shown as mean ± SD from two independent experiments with triplicates. See also Figure S5.

upstream of mir-145 transcriptional start site (Figure S5D). Quantitative RT-PCR confirmed that FoxO3 activation can significantly upregulate mir-145 expression in RCC4 cells (Figure 6E). Conversely, knockdown of FoxO1 and FoxO3 in UOK101 cells led to decrease of mir-145 and Mxi1-SRα expression, and increase of Myc expression (Figure 6F). Furthermore, chromatin immunoprecipitation (ChIP) analysis documented that both ectopically expressed and endogenous FoxO1 and FoxO3 can directly bind to both FoxO BEs in mir-145 promoter region (Figure 6G; Figure S5E). Importantly, knockdown of mir-145 by anti-mir-145 (Figure S5F) significantly normalized Myc expression on FoxO activation (Figure 6H), strongly suggesting that mir-145 contributes to FoxO-mediated suppression of Myc expression in RCC cells. Consistent with recent report in other cell types (Sachdeva et al., 2009), we found overexpression of mir-145 was sufficient to downregulate Myc expression (Figure S5G and S5H) and inhibit cell growth in RCC4 cells (Figure S5I). Finally, knockdown of Mxi1-SRα, knockdown of mir-145, and overexpression of Myc, either individually or in combination, can significantly rescue the cell growth inhibition effected by FoxO activation in RCC4 cells (Figure 6I). Together, these data establish that FoxO inhibits both Myc activity and expression via transcriptional regulation of Mxi1-SRα and mir-145, and that Myc signaling is at least one key downstream effector of FoxO in RCC cells.

Myc/Mxi1-SRα/mir-145 Alterations in *Tsc1* Renal Cancer Mouse Models and Human RCCs

The above mechanistic studies in renal cancer cell culture systems prompted further investigation of Myc signaling in vivo in the context of RCC development in mice and humans. Examination of Myc/Mxi1-SRα/mir-145 status in *Tsc1* mouse models revealed that mir-145 and Mxi1-SRα expression levels were upregulated in *Tsc1* KO polycystic kidneys (with FoxO activation) and downregulated in *Tsc1* KO kidney tumors (with FoxO extinction) compared with *Tsc1* WT kidneys (Figure 7A). Furthermore, although Myc expression was downregulated in *Tsc1* KO polycystic kidneys compared with *Tsc1* WT kidneys (Figure 7A), there was no obvious difference in Myc protein levels and in expression levels of Myc targets between *Tsc1* KO polycystic kidneys and *Tsc1* WT kidneys (Figures 7B and 7C). Myc expression and protein levels, and Myc target expression levels, are dramatically increased in *Tsc1* KO kidney tumors compared with either *Tsc1* WT kidneys or *Tsc1* KO polycystic kidneys (Figures 7A–7C). Because mTORC1 hyperactivation is also known to promote Myc translation (West et al., 1998), our data together suggest that, in *Tsc1* KO polycystic kidneys with mTORC1 hyperactivation and FoxO activation, Myc protein level is balanced by both increased protein synthesis afforded by mTORC1 hyperactivation and decreased mRNA levels via FoxO activation. While in *Tsc1* KO kidney tumors, loss of FoxO expression leads to increased Myc expression. This, together with increased protein synthesis, leads to further increased Myc protein level, which contributed to the renal tumorigenesis in *Tsc1* KO mice.

Examination of Myc/Mxi1-SRα/mir-145 status in human RCCs in published human RCC transcriptome data set (including 11 normal kidney samples and 59 ccRCC samples) (Beroukhim et al., 2009) revealed that Myc expression was significantly upregulated in ccRCCs compared with normal kidneys (Figure 7D;

p = 7.42×10^{-9}), correlating with aforementioned data that FoxO1/3 are extinguished in the majority of human ccRCC samples. Further computational analyses revealed that the mean expression levels of Myc signature genes (the same signature genes used in our FoxO RCC transcriptome analysis in Figure 5C) were significantly upregulated in ccRCCs compared with normal kidneys (Figure S6A) (p = 4.12×10^{-11}) and that the expression levels of Myc positively correlated with the mean expression levels of Myc signature genes in ccRCC and normal kidney samples (Figure 7E; Pearson correlation coefficient: 0.61, p = 2.03×10^{-8}), strongly suggesting that Myc signaling is also upregulated in ccRCCs. We also performed RT-qPCR experiments to examine the expression levels of Myc, selected Myc targets (CCND2, GADD45A, LDHA, HK2, and ENO1), mir-145, and Mxi1-SRα in 12 human ccRCC and matched normal kidney samples. These experiments confirmed upregulation of Myc, CCND2, LDHA, HK2, and ENO1, but downregulation of mir-145, Mxi1-SRα, and GADD45A (Myc-repressed target) in ccRCC compared with matched normal kidney samples (Figures 7F–7H; Figures S6B–S6F). Together, our data strongly suggests that FoxO regulation of Myc/Mxi1-SRα/mir-145 signaling network plays a role in suppressing renal tumorigenesis in *Tsc1* renal tumor mouse model and human RCCs (Figure 7I).

DISCUSSION

The mTORC1-mediated negative feedback regulation of PI3K-AKT (Shaw and Cantley, 2006), cancer type-specific nature of PI3K-AKT pathway signaling in vivo, and the multiple AKT downstream effectors in cancer (Manning and Cantley, 2007) prompted us to define mTORC1 circuitry on the genetic, genomic, and biological levels in RCC pathogenesis. By using genetically defined mice and human RCC cell line models, this study establishes that FoxOs play a critical role in an mTORC1-directed negative feedback circuit in the context of renal tumorigenesis. FoxO1 and FoxO3 are robustly activated in *Tsc1*-deficient benign polycystic neoplasias as well as *Tsc1* KO MEFs, and consistently extinguished on progression to renal adenomas and carcinomas. In addition, combined deletion of *Tsc1* and *FoxO1/3/4* provoked dramatic exacerbation of the renal tumor phenotypes, establishing activated FoxO signaling as a potent block in *Tsc1* null renal cancer development.

In elucidating the biological mechanisms by which loss of *FoxO* serves to promote *Tsc1* null renal cancer development, we provide evidence that knockdown of FoxO in RCC cells leads to increased Myc expression and enhanced cell proliferation, supporting a model that loss of *FoxO* and subsequent Myc activation function to promote cell cycling at the transition from premalignant polycystic kidney epithelial cells to adenoma in *Tsc1* mice. In addition, although FoxO is a key progression factor, we acknowledge that loss of *FoxO* (and *Tsc1* LOH) may represent one of several genetic networks commandeered in the course of kidney tumorigenesis, a view consistent with lengthy renal tumor latency in our *Tsc1*$^{+/-}$ *FoxO*$^{-/-}$ mice. Thus, this model system may serve as a foundation for identification of cooperative genetic events involved in renal tumorigenesis.

The FoxO family members serve as redundant tumor suppressors in vivo, and FoxO1 and FoxO3 exert the major tumor suppressor activity (Paik et al., 2007). Correspondingly, we
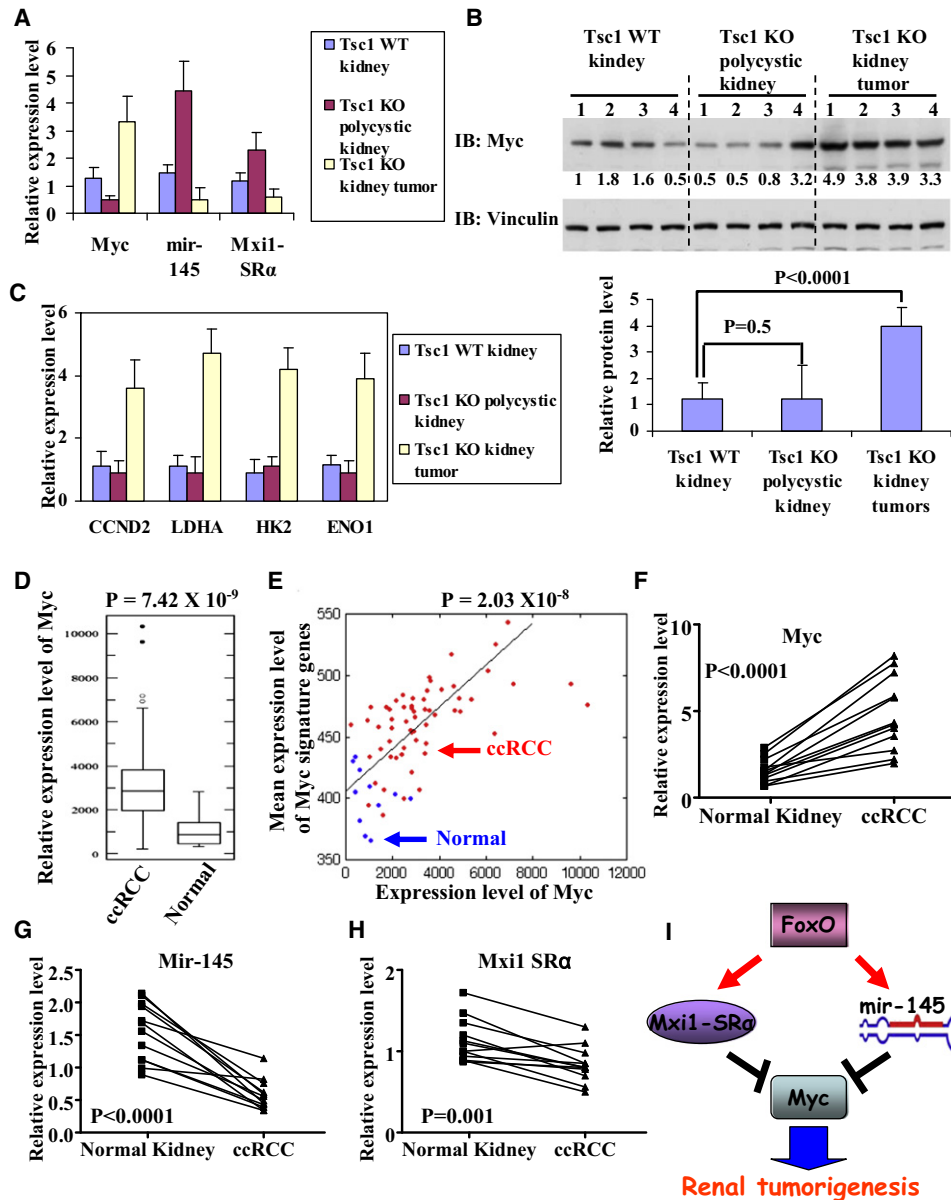
Figure 7. Myc/Mxi1-SRα/mir-145 Alterations in *Tsc1* Renal Cancer Mouse Models and Human RCCs

(A) Bar graphs showing relative expression levels of Myc, Mxi1-SRα, mir-145 in *Tsc1* WT kidneys, *Tsc1* KO polycystic kidneys, and *Tsc1* KO kidney tumors. Four samples were analyzed in each setting. p < 0.01 for comparison between *Tsc1* WT kidneys and *Tsc1* KO polycystic kidneys (or *Tsc1* KO kidney tumors) for each gene. Data are shown as mean ± SD.

(B) Western blotting showing Myc and Vinculin protein levels in *Tsc1* WT kidneys, *Tsc1* KO polycystic kidneys, and *Tsc1* KO kidney tumors. Quantified Myc protein levels are also shown in the bar graph. Data are shown as mean ± SD.

(C) Bar graphs showing relative expression levels of Myc targets in *Tsc1* WT kidneys, *Tsc1* KO polycystic kidneys, and *Tsc1* KO kidney tumors. Four samples were analyzed in each setting. p > 0.05 for comparison between *Tsc1* WT kidneys and *Tsc1* KO polycystic kidneys for each gene. p < 0.01 for comparison between *Tsc1* WT kidneys (or *Tsc1* KO polycystic kidneys) and *Tsc1* KO kidney tumors. Data are shown as mean ± SD.

(D) Box-plots showing Myc expression levels in ccRCC and normal kidney samples.

(E) Positive correlation between expression levels of Myc and Myc signature genes in ccRCC and normal kidney samples. x axis: expression levels of Myc; y axis: mean expression levels of Myc signature genes; blue spots: normal kidney sample; red spots: ccRCC sample.

(F–H) The relative expression levels of Myc, Mxi1-SRα, mir-145 in 12 ccRCC samples, and matched normal kidney samples.

(I) FoxO inhibits Myc activity via transcriptional upregulation of Mxi1-SRα and downregulates Myc mRNA level via transcriptional upregulation of mir-145. Myc signaling is the key downstream effector of FoxO to suppress renal tumorigenesis. See also Figure S6.

observed that FoxO1 and FoxO3 are always co-extinguished in *Tsc1*-deficient mouse renal tumors and human renal tumors, suggesting that both FoxOs need to be eliminated to bypass FoxO-mediated checkpoint. Furthermore, activation of FoxO1 and FoxO3 in human renal cancer cells resulted in similar cellular phenotypes (apoptosis and cell cycle arrest) and transcriptomic

alterations (such as inhibition of Myc expression). Thus, we conclude that FoxO1 and FoxO3 function as redundant tumor suppressors in renal tumorigenesis.

In this study, we found FoxO1 and FoxO3 levels are extinguished in the majority of the aggressive subtypes of human RCC, including clear cell and papillary tumors, but maintained or robustly activated in less aggressive carcinomas (i.e., chromophobe RCC) and benign tumors. The underlying mechanisms responsible for such differential expression/activation patterns of FoxOs in different kidney tumor types are not understood currently. It is worth noting that recent oncogenomic analysis identified frequent hemizygous deletions at 13q in human clear cell RCC samples, and *FoxO1* was identified as a downregulated gene in the minimal common region of the 13q deletion (Kojima et al., 2010), suggesting that genomic alteration might be at least a contributing mechanism for the loss of FoxO1 staining in our analysis. We speculate that other mechanisms operating on the epigenetic and posttranslational levels might be also involved in effecting extinction of FoxO expression/activity in these RCC samples.

Our integrated transcriptomic, computational, and functional studies identified Myc-Mxi1 signaling as the key downstream effector of FoxOs in the regulation of renal cancer cell proliferation. This finding is particularly intriguing in light of our previous work showing that deletion of *Mxi1* in mice led to the development of polycystic kidney disease (PKD) similar to the PKD observed in *Tsc1*-deficient mice (Schreiber-Agus et al., 1998). Notably, Myc transgenic mice also developed PKD (Trudel et al., 1991). These mouse genetic studies thus provide important complementary evidence to our computational and functional analyses in support of the critical function of Myc-Mxi1 signaling in mTORC1-FoxO-directed renal tumorigenesis.

Myc and Mxi1 are also highly relevant to human RCC. Recent oncogenomic profiles show that *Myc* is amplified in about 12% clear cell RCC samples and is the only gene in the 8q amplification peak region, confirming Myc as an oncogene in human kidney cancer (Beroukhim et al., 2009). Furthermore, *Mxi1* locus is subjected to homozygous and hemizygous deletion in a subset of clear cell RCC samples (Beroukhim et al., 2009), suggesting that Mxi1 functions as a tumor suppressor in human kidney cancer. Mechanistically, it has been shown that Myc can crosstalk with HIF signaling to regulate cell cycle entry, metabolism, and mitochondrial biogenesis in RCC cells (Dang et al., 2008; Gordan et al., 2007a, 2007b; Zhang et al., 2007). Further study will be necessary to investigate whether FoxO can regulate cancer cell metabolism and mitochondrial biogenesis in the context of renal tumorigenesis via Myc signaling.

Finally, our data also point to combination therapeutic regimens for improved treatment of renal cancer. Specifically, because our study demonstrated that FoxOs are extinguished in the majority of human RCC samples and serve as an critical tumor suppressor axis in renal cancer, it predicts that mTORC1 inhibition (or mTORC1/PI3K inhibition) would not affect the downstream oncogenic effect afforded by loss of FoxO, which explains, at least in part, why mTORC1 inhibition has relatively limited impact on kidney cancer patients. Our study further suggests combination therapy by mTORC1 inhibition and a FoxO restabilization/activation and/or Myc destabilization strategy might provide improved treatment in kidney cancer. As discussed above, currently we favor a model that FoxO extinction in human RCC might result from posttranslational mechanism (such as phosphorylation-mediated protein degradation). Further understanding of how FoxOs are extinguished in human RCC might therefore provide treatment strategies in RCC, including such strategies as blocking Crm1-mediated nuclear export. Alternatively, our study suggests that combined inhibition of mTORC1 and Myc signaling might further improve the treatment of kidney cancer. Interference of Myc signaling may be provided by current efforts to target Myc heterodimerization with Max or by targeting factors regulating Myc protein degradation.

In summary, this integrated genetic, transcriptomic, computational, and cell biological study has provided additional insights into the molecular basis of mTORC1-mediated negative feedback in the context of renal tumorigenesis. Our study identifies FoxO transcription factors as a critical checkpoint that functions to constrain mTORC1-mediated renal tumorigenesis and serves as a tumor suppressor axis in renal cancer. Further study of the FoxO network may illuminate additional points of therapeutic intervention and provide pharmacodynamic markers for guiding the development of agents targeting components of the PI3K pathway in RCC patients.

EXPERIMENTAL PROCEDURES

Generation and Analysis of Mice

The *Rosa26-CreERT2* mice (Vooijs et al., 2001) were mated with *FoxO1/3/4$^{L/L}$* mice (Paik et al., 2007) to generate *FoxO1/3/4$^{L/L}$*, *Rosa26-CreERT2* mice, which were then crossed with *Tsc1$^{L/L}$* mice (Kwiatkowski et al., 2002) to generate various mice lines with desired genotypes. All cohorts were in a FVB/n, C57Bl/6, and 129/Sv mixed genetic background. Littermates at 4–5 weeks of age were treated daily by intraperitoneal injection of tamoxifen in corn oil (0.13 mg/g body weight) for 5 consecutive days (Gan et al., 2008). The tamoxifen was intended to induce CreERT2 translocation into the nucleus, thereby leading to transient Cre-mediated recombination. Overall survival, as well as spontaneous formation of tumors, was monitored in various cohorts. Animals were autopsied and all tissues were examined regardless of their pathological status. All animal manipulations were performed with Harvard's and Dana-Farber Cancer Institute's Institutional Animal Care and Use Committee (IACUC) approval.

Human Samples

Human RCC TMA and RNA samples were obtained from Renal Cancer Tissue Acquisition, Pathology, and Clinical Data Core (TAPCD) at Dana-Farber/Harvard Cancer Center (DF/HCC) Kidney Cancer SPORE directed by S.S. All patients provided informed consent and the study was approved by the Institutional Review Boards of Dana-Farber Cancer Institute and DF/HCC Renal Cancer TAPCD Core Utilization Committee (RCTUC).

Antibodies for Immunohistochemistry and Western Blot Analysis

The following antibodies were used: Vinculin (Sigma), Myc (sc-42, Santa Cruz, to detect endogenous Myc), Myc (9E10, Santa Cruz, to detect Myc tag), S6K (Santa Cruz), TSC1, FoxO1 (C29H4), FoxO3 (75D8), FoxO4, Thr24 phospho-FoxO1/Thr32 FoxO3, AKT, Ser473 phospho AKT, S6, Ser240/244 phospho-S6, Thr389 phospho-S6K, PARP, and cleaved-Caspase 3 (all from Cell Signaling Technology).

Constructs and Reagents

FoxO1(TA) and FoxO3(TA) cDNAs were obtained from addgene, and then were fused with Myc-tagged ERT2 at C terminus and cloned in retroviral vector pBabe. Myc expression construct is described in our recent publication (Zheng et al., 2008). Lentiviral shRNA vectors targeting human Mxi1 and non-targeting control construct shGFP were obtained from the RNAi Consortium at

the Dana-Farber/Broad Institute. Lentiviral mir-145 expression vector was purchased from System Biosciences. Anti-mir-145 and scrambled oligos were ordered from Exiqon.

Cell Culture Studies

Immortalized human kidney cells (HK2), human kidney cancer cell lines used in this study, and human embryonic kidney cell line HEK293T were purchased from American Type Culture Collection (ATCC). Lentiviruses or retroviruses were produced in HEK293T cells with packing mix (ViraPower Lentiviral Expression System, Invitrogen) and used to infect target cells as per manufacturer's instruction. To reactivate FoxO, FoxO1(TA)ERT2 or FoxO3(TA)ERT2 cells were treated with 100 nM 4OHT or vehicle for different periods of time as indicated and subjected to various analyses. Cell proliferation assays were performed in 12-well plates in triplicate with 10,000 cells per well. Cells were fixed in 10% formalin in PBS, and stained with crystal violet at different days as indicated. At the conclusion of the assay, crystal violet was extracted with 10% acetic acid and absorbance at 595 nm was measured with 96-well plate reader.

ChIP Analysis

Chip experiment was performed using EZ-Chip Kit (Chemicon) as per manufacturer's instruction.

Expression Profiling and Quantitative Real-Time PCR Analysis

Details of expression profiling and quantitative real-time PCR analysis are provided in Supplemental Experimental Procedures.

Statistical Analysis

Tumor-free survivals were analyzed using GraphPad Prism4. Statistical analyses were performed using nonparametric Mann-Whitney test. Comparisons of cell growth and gene expression were performed using the unpaired Student's t test. For all experiments with error bars, standard deviation was calculated to indicate the variation within each experiment and data, and values represent mean ± standard error of mean.

ACCESSION NUMBERS

Completed microarray data have been deposited in the Gene Expression Omnibus website with accession code GSE23926.

SUPPLEMENTAL INFORMATION

Supplemental Information includes Supplemental Experimental Procedures, Supplemental References, six figures, and one table and can be found with this article online at doi:10.1016/j.ccr.2010.10.019.

REFERENCES

Accili, D., and Arden, K.C. (2004). FoxOs at the crossroads of cellular metabolism, differentiation, and transformation. Cell *117*, 421–426.

Algaba, F. (2008). Renal adenomas: pathological differential diagnosis with malignant tumors. Adv. Urol., 974848. Epub 2008 Oct 8.

Alland, L., Muhle, R., Hou, H., Jr., Potes, J., Chin, L., Schreiber-Agus, N., and DePinho, R.A. (1997). Role for N-CoR and histone deacetylase in Sin3-mediated transcriptional repression. Nature *387*, 49–55.

Atkins, M.B., Hidalgo, M., Stadler, W.M., Logan, T.F., Dutcher, J.P., Hudes, G.R., Park, Y., Liou, S.H., Marshall, B., Boni, J.P., et al. (2004). Randomized phase II study of multiple dose levels of CCI-779, a novel mammalian target of rapamycin kinase inhibitor, in patients with advanced refractory renal cell carcinoma. J. Clin. Oncol. *22*, 909–918.

Ayer, D.E., Lawrence, Q.A., and Eisenman, R.N. (1995). Mad-Max transcriptional repression is mediated by ternary complex formation with mammalian homologs of yeast repressor Sin3. Cell *80*, 767–776.

Beroukhim, R., Brunet, J.P., Di Napoli, A., Mertz, K.D., Seeley, A., Pires, M.M., Linhart, D., Worrell, R.A., Moch, H., Rubin, M.A., et al. (2009). Patterns of gene expression and copy-number alterations in von-Hippel Lindau disease-associated and sporadic clear cell carcinoma of the kidney. Cancer Res. *69*, 4674–4681.

Bhaskar, P.T., and Hay, N. (2007). The two TORCs and Akt. Dev. Cell *12*, 487–502.

Bild, A.H., Yao, G., Chang, J.T., Wang, Q., Potti, A., Chasse, D., Joshi, M.B., Harpole, D., Lancaster, J.M., Berchuck, A., et al. (2006). Oncogenic pathway signatures in human cancers as a guide to targeted therapies. Nature *439*, 353–357.

Cai, S.L., and Walker, C.L. (2006). TSC2, a key player in tumor suppression and cystic kidney disease. Nephrol. Ther. *2* (*Suppl 2*), S119–S122.

Cohen, H.T., and McGovern, F.J. (2005). Renal-cell carcinoma. N. Engl. J. Med. *353*, 2477–2490.

Cully, M., You, H., Levine, A.J., and Mak, T.W. (2006). Beyond PTEN mutations: the PI3K pathway as an integrator of multiple inputs during tumorigenesis. Nat. Rev. Cancer *6*, 184–192.

Dang, C.V., Kim, J.W., Gao, P., and Yustein, J. (2008). The interplay between MYC and HIF in cancer. Nat. Rev. Cancer *8*, 51–56.

Delpuech, O., Griffiths, B., East, P., Essafi, A., Lam, E.W., Burgering, B., Downward, J., and Schulze, A. (2007). Induction of Mxi1-SR alpha by FOXO3a contributes to repression of Myc-dependent gene expression. Mol. Cell. Biol. *27*, 4917–4930.

Eilers, M., and Eisenman, R.N. (2008). Myc's broad reach. Genes Dev. *22*, 2755–2766.

Gan, B., Sahin, E., Jiang, S., Sanchez-Aguilera, A., Scott, K.L., Chin, L., Williams, D.A., Kwiatkowski, D.J., and DePinho, R.A. (2008). mTORC1-dependent and -independent regulation of stem cell renewal, differentiation, and mobilization. Proc. Natl. Acad. Sci. USA *105*, 19384–19389.

Gordan, J.D., Bertout, J.A., Hu, C.J., Diehl, J.A., and Simon, M.C. (2007a). HIF-2alpha promotes hypoxic cell proliferation by enhancing c-myc transcriptional activity. Cancer Cell *11*, 335–347.

Gordan, J.D., Thompson, C.B., and Simon, M.C. (2007b). HIF and c-Myc: sibling rivals for control of cancer cell metabolism and proliferation. Cancer Cell *12*, 108–113.

Greer, E.L., and Brunet, A. (2005). FOXO transcription factors at the interface between longevity and tumor suppression. Oncogene *24*, 7410–7425.

Guertin, D.A., and Sabatini, D.M. (2007). Defining the role of mTOR in cancer. Cancer Cell *12*, 9–22.

Hanna, S.C., Heathcote, S.A., and Kim, W.Y. (2008). mTOR pathway in renal cell carcinoma. Expert Rev. Anticancer Ther. *8*, 283–292.

Hay, N., and Sonenberg, N. (2004). Upstream and downstream of mTOR. Genes Dev. *18*, 1926–1945.

Heinzel, T., Lavinsky, R.M., Mullen, T.M., Soderstrom, M., Laherty, C.D., Torchia, J., Yang, W.M., Brard, G., Ngo, S.D., Davie, J.R., et al. (1997).

A complex containing N-CoR, mSin3 and histone deacetylase mediates transcriptional repression. Nature 387, 43–48.

Huang, J., and Manning, B.D. (2008). The TSC1-TSC2 complex: a molecular switchboard controlling cell growth. Biochem. J. 412, 179–190.

Hudes, G., Carducci, M., Tomczak, P., Dutcher, J., Figlin, R., Kapoor, A., Staroslawska, E., Sosman, J., McDermott, D., Bodrogi, I., et al. (2007). Temsirolimus, interferon alfa, or both for advanced renal-cell carcinoma. N. Engl. J. Med. 356, 2271–2281.

Inoki, K., Corradetti, M.N., and Guan, K.L. (2005). Dysregulation of the TSC-mTOR pathway in human disease. Nat. Genet. 37, 19–24.

Kobayashi, T., Minowa, O., Sugitani, Y., Takai, S., Mitani, H., Kobayashi, E., Noda, T., and Hino, O. (2001). A germ-line Tsc1 mutation causes tumor development and embryonic lethality that are similar, but not identical to, those caused by Tsc2 mutation in mice. Proc. Natl. Acad. Sci. USA 98, 8762–8767.

Kojima, T., Shimazui, T., Horie, R., Hinotsu, S., Oikawa, T., Kawai, K., Suzuki, H., Meno, K., Akaza, H., and Uchida, K. (2010). FOXO1 and TCF7L2 genes involved in metastasis and poor prognosis in clear cell renal cell carcinoma. Genes Chromosomes Cancer 49, 379–389.

Kwiatkowski, D.J., and Manning, B.D. (2005). Tuberous sclerosis: a GAP at the crossroads of multiple signaling pathways. Hum. Mol. Genet. 14 Spec No. 2, R251–R258.

Kwiatkowski, D.J., Zhang, H., Bandura, J.L., Heiberger, K.M., Glogauer, M., el-Hashemite, N., and Onda, H. (2002). A mouse model of TSC1 reveals sex-dependent lethality from liver hemangiomas, and up-regulation of p70S6 kinase activity in Tsc1 null cells. Hum. Mol. Genet. 11, 525–534.

Li, Y., Corradetti, M.N., Inoki, K., and Guan, K.L. (2004). TSC2: filling the GAP in the mTOR signaling pathway. Trends Biochem. Sci. 29, 32–38.

Linehan, W.M., and Zbar, B. (2004). Focus on kidney cancer. Cancer Cell 6, 223–228.

Lopez-Beltran, A., Scarpelli, M., Montironi, R., and Kirkali, Z. (2006). 2004 WHO classification of the renal tumors of the adults. Eur. Urol. 49, 798–805.

Luo, J., Manning, B.D., and Cantley, L.C. (2003). Targeting the PI3K-Akt pathway in human cancer: rationale and promise. Cancer Cell 4, 257–262.

Ma, X.M., and Blenis, J. (2009). Molecular mechanisms of mTOR-mediated translational control. Nat. Rev. Mol. Cell Biol. 10, 307–318.

Manalo, D.J., Rowan, A., Lavoie, T., Natarajan, L., Kelly, B.D., Ye, S.Q., Garcia, J.G., and Semenza, G.L. (2005). Transcriptional regulation of vascular endothelial cell responses to hypoxia by HIF-1. Blood 105, 659–669.

Manning, B.D. (2004). Balancing Akt with S6K: implications for both metabolic diseases and tumorigenesis. J. Cell Biol. 167, 399–403.

Manning, B.D., and Cantley, L.C. (2007). AKT/PKB signaling: navigating downstream. Cell 129, 1261–1274.

Motzer, R.J., Escudier, B., Oudard, S., Hutson, T.E., Porta, C., Bracarda, S., Grunwald, V., Thompson, J.A., Figlin, R.A., Hollaender, N., et al. (2008). Efficacy of everolimus in advanced renal cell carcinoma: a double-blind, randomised, placebo-controlled phase III trial. Lancet 372, 449–456.

Paik, J.H., Kollipara, R., Chu, G., Ji, H., Xiao, Y., Ding, Z., Miao, L., Tothova, Z., Horner, J.W., Carrasco, D.R., et al. (2007). FoxOs are lineage-restricted redundant tumor suppressors and regulate endothelial cell homeostasis. Cell 128, 309–323.

Pantuck, A.J., Seligson, D.B., Klatte, T., Yu, H., Leppert, J.T., Moore, L., O'Toole, T., Gibbons, J., Belldegrun, A.S., and Figlin, R.A. (2007). Prognostic relevance of the mTOR pathway in renal cell carcinoma: implications for molecular patient selection for targeted therapy. Cancer 109, 2257–2267.

Rini, B.I., Campbell, S.C., and Escudier, B. (2009). Renal cell carcinoma. Lancet 373, 1119–1132.

Robb, V.A., Karbowniczek, M., Klein-Szanto, A.J., and Henske, E.P. (2007). Activation of the mTOR signaling pathway in renal clear cell carcinoma. J. Urol. 177, 346–352.

Sabatini, D.M. (2006). mTOR and cancer: insights into a complex relationship. Nat. Rev. Cancer 6, 729–734.

Sachdeva, M., Zhu, S., Wu, F., Wu, H., Walia, V., Kumar, S., Elble, R., Watabe, K., and Mo, Y.Y. (2009). p53 represses c-Myc through induction of the tumor suppressor miR-145. Proc. Natl. Acad. Sci. USA 106, 3207–3212.

Salmena, L., Carracedo, A., and Pandolfi, P.P. (2008). Tenets of PTEN tumor suppression. Cell 133, 403–414.

Samuels, Y., Wang, Z., Bardelli, A., Silliman, N., Ptak, J., Szabo, S., Yan, H., Gazdar, A., Powell, S.M., Riggins, G.J., et al. (2004). High frequency of mutations of the PIK3CA gene in human cancers. Science 304, 554.

Schreiber-Agus, N., Chin, L., Chen, K., Torres, R., Rao, G., Guida, P., Skoultchi, A.I., and DePinho, R.A. (1995). An amino-terminal domain of Mxi1 mediates anti-Myc oncogenic activity and interacts with a homolog of the yeast transcriptional repressor SIN3. Cell 80, 777–786.

Schreiber-Agus, N., Meng, Y., Hoang, T., Hou, H., Jr., Chen, K., Greenberg, R., Cordon-Cardo, C., Lee, H.W., and DePinho, R.A. (1998). Role of Mxi1 in ageing organ systems and the regulation of normal and neoplastic growth. Nature 393, 483–487.

Shaw, R.J., and Cantley, L.C. (2006). Ras, PI(3)K and mTOR signalling controls tumour cell growth. Nature 441, 424–430.

Trudel, M., D'Agati, V., and Costantini, F. (1991). C-myc as an inducer of polycystic kidney disease in transgenic mice. Kidney Int. 39, 665–671.

Um, S.H., D'Alessio, D., and Thomas, G. (2006). Nutrient overload, insulin resistance, and ribosomal protein S6 kinase 1, S6K1. Cell Metab. 3, 393–402.

Vooijs, M., Jonkers, J., and Berns, A. (2001). A highly efficient ligand-regulated Cre recombinase mouse line shows that LoxP recombination is position dependent. EMBO Rep. 2, 292–297.

West, M.J., Stoneley, M., and Willis, A.E. (1998). Translational induction of the c-myc oncogene via activation of the FRAP/TOR signalling pathway. Oncogene 17, 769–780.

Wullschleger, S., Loewith, R., and Hall, M.N. (2006). TOR signaling in growth and metabolism. Cell 124, 471–484.

Zhang, H., Gao, P., Fukuda, R., Kumar, G., Krishnamachary, B., Zeller, K.I., Dang, C.V., and Semenza, G.L. (2007). HIF-1 inhibits mitochondrial biogenesis and cellular respiration in VHL-deficient renal cell carcinoma by repression of C-MYC activity. Cancer Cell 11, 407–420.

Zheng, H., Ying, H., Yan, H., Kimmelman, A.C., Hiller, D.J., Chen, A.J., Perry, S.R., Tonon, G., Chu, G.C., Ding, Z., et al. (2008). p53 and Pten control neural and glioma stem/progenitor cell renewal and differentiation. Nature 455, 1129–1133.